J. Infrastructure Plan. and Man., JSCE, No.620/V-43, 303-314, 1999 May

TWO DIMENSIONAL ELASTIC ANALYSIS FOR ASPHALT MIXTURE ON STEEL PLATE

Shoichi AKIBA[1], Yuzou KURIYAGAWA[2], Sumio G. NOMACHI[3] and Narioki AKIYAMA[4]

[1] Member of JSCE, Dr. Eng., Research Associate, Department of Civil Engineering, Nihon University (Izumi 1-2-1,Narasino, Chiba 275-8575, Japan)
[2] Member of JSCE, Dr. Eng., Associate Professor, Department of Civil Engineering, Nihon University (Izumi 1-2-1,Narasino, Chiba 275-8575, Japan)
[3] Member of JSCE, Dr. Eng., Professor Emeritus, Hokkaido University (Sakaecho 2-2-5, Kitahiroshima, Hokkaido 061-1133, Japan)
[4] Member of JSCE, Dr. Eng., Professor, Department of Civil Engineering, Nihon University (Izumi 1-2-1,Narasino, Chiba 275-8575, Japan)

This paper is intended to report the results of the two-dimensional elastic analysis for test specimens consisting of two layers: an asphalt mixture to which the beam theory is inapplicable due to its low stiffness, and a thin steel plate on which the mixture is placed. Then, numerical computation has provided the authors with valuable data and information, such as the sizes and shapes of test specimens, friction between the upper and the lower layers, and the stiffness ratio between the two layers. All of these are essential factors in determining the mechanical property of a mixture by using the results of displacement measurement for the purpose of evaluating the elasticity of a pavement mixture.

Key Words : bending test, two dimensional elastic analysis, low stiffness, steel plate, surface displacement, spacemen size

1. INTRODUCTION

The prediction of the service life of pavements is based for the most part on the evaluation of various factors associated with durability, such as fatigue strength resistance and flow ability resistance, of a pavement mixture which contains bitumen material in most cases [1)-3)]. The laboratory evaluation of the fatigue strength and elasticity of the mixture, in particular, relies on repeated bending tests, although testing methods have yet to be further investigated to solve the problems arising in this type of test [4)].

The present authors are proposing a method of determining the mechanical property associated with the elasticity of asphalt mixture by using solutions to the elastic problems of displacement components, which can be obtained through two-dimensional elastic analysis, and displacement measurements in repeated bending tests. When the specimens employed for the testing are larger than normal size, this method lends itself to facilitating a more rational evaluation of the fatigue and elasticity of a mixture [5)-7)]. And yet the proposed method has been found to be less than effective in evaluating the mechanical property of the material when its stiffness is low (i.e., when its temperature is high), whereas the method has proved to be applicable when the stiffness of the material is sufficiently high (i.e., when its temperature is low). This is due to the fact that a degree of deflection by self-weight under a no-loading condition changes over time because of the viscoelasticity of asphalt, thereby making it extremely difficult to maintain a stable status before loading. Accordingly, the effect of deflection whose degrees vary over time must be removed in employing this method for the evaluation of pavement materials with low stiffness.

In an effort to find a solution to the problem, Himeno et al. conducted a series of repeated bending tests on a beam-shaped test specimen of asphalt mixture (4cm×4cm×30cm) that was placed on a steel plate [3)]. This type of approach for evaluating the fatigue strength of asphalt mixture by the use of a two-layer specimen has been proved to be highly effective in expanding the applicability of the repeated bending test, so that it will be adopted for evaluating elasticity, viscoelastity and other aspects of the durability of

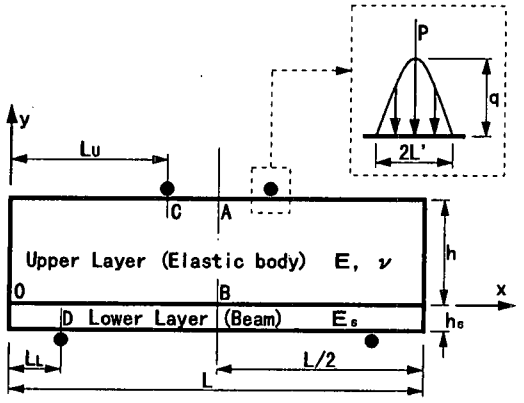

Fig.1 Analyzed beam model with unit width under symmetrical loads with parabolic distribution.

materials characterized by low stiffness. Furthermore, this specific approach is expected to be useful in evaluating asphalt mixture on steel decks. Problems yet remain unsolved in some respects, including deflection measurements required for evaluation, the bonding of asphalt mixture and a steel plate, and applicability of analysis results based on the beam theory, as well as problems on the shapes and sizes of test specimens as posed by the authors [5)-7)]. This paper describes investigations by means of two-dimensional elastic analysis of a beam of two-layered structure under bending load. The analysis was carried out by using the above-mentioned test method in combination with larger-than-conventional sizes of test specimens, with a view to determining the mechanical property required for evaluating the elasticity of an asphalt mixture with low stiffness. For the sake of practicality, and because the use of a personal computer was preferred in order to shorten calculation time, an analysis model was produced by using an elastic material for the upper layer of the asphalt mixture, while a straight steel beam with higher rigidity was used for the lower part. For setting the load and the continuous conditions of displacement for the interface between the upper and lower layers, the differential equation [8)] of the beam theory was adopted. In contrast to the elastic analysis of a two-layered structure consisting of elastic materials only, this method of using both elastic and rigid materials in a model structure produces approximate results. Consequently, this analysis method entailed discussions on the applicability of the analysis results to confirm the usefulness of the analysis method. The discussions were followed by calculations for examining the effect of the sizes and shapes of specimens and the bonding conditions of the upper and the lower layers on deflection to be analyzed, as clarification of such effects are essential for determining the mechanical property of asphalt mixture. Some calculations were also carried out to delve for factors that might influence stress in horizontal direction when mechanical property was determined on the basis of analysis results of stress in horizontal direction and strain measurements.

2. TWO - DIMENSIONAL ELASTIC ANALYSIS

(1) Equations for Displacement and Stress Components

Stress components in horizontal direction x and vertical direction y and shearing stress are denoted by σ_x, σ_y and τ_{xy}, respectively, while displacement components in x and y directions are denoted by u and v. For the elastic analysis related to the problems of boundary values of plane stress, a method of the finite Fourier transforms that had been publicized by Nomachi [9)] was adopted. Since the authors have already derived elasticity solutions of stress and displacement components, releasing a paper describing the actual use of this method [5)-7)], no explanations are deemed necessary here concerning the solutions and processes for deriving them.

The use of the above-mentioned solutions makes it possible to analyze the stress and displacement of two-layered structure of elastic materials. In case of the two layers, however, number of unknown squarely increase, and it results in much more CPU time on the level of the personal computer. Because the elastic material for the lower layer of the specimen takes the form of a long, thin beam, an increase in the number of terms of series causes overflow in floating point computation for a mathematical function in the programming software, preventing accurate calculation results from being produced. It should be noted that the researches being reported in this paper aimed to identify the behavior of stress and displacement of a test specimen whose upper layer was assumed to be made of elastic material. In other words, it was not necessary to examine the elastic behavior of the materials of the lower layer, since the elastic property of the material was supposed to be known.

In view of the above, a model was constructed assuming that the lower layer of the specimen was a straight beam, instead of using the analysis method for a test specimen in which elastic

materials are used for both the upper and the lower layers. Analysis of the stress to the lower layer and the continuity conditions of displacement was carried out through the differential equation of the beam theory [8]. As mentioned above, for simplification purposes, the lower layer takes the form of a straight beam. Since no significant difference in flexural rigidity is observed between the upper layer and the lower layer, it can be assumed that the resistance to bending deformation is caused by the two layers being combined. Accordingly, the beam discussed in this paper is defined as a two-layered structure beam.

According to **Fig. 1**, which indicates the bending test model of elastic material on a long, thin beam, boundary conditions can be represented by Equations (1) to (3). For Equation (3), however, there are two cases: when no friction is observed over the interface (CASE I) and when friction takes place over the interface (CASE II).

When $x=0,L$ $\sigma_x)_{x=L}=\sigma_x)_{x=0}=0$, $\tau_{xy})_{x=L}=\tau_{xy})_{x=0}=0$, $v)_{x=L}=v)_{x=0}$ (1)

When $y=h$ $\sigma_y)_{y=h}=P_U(x)$, $\tau_{xy})_{y=h}=0$ (2)

When $y=0$ CASE I $\tau_{xy})_{y=0}=0$

CASE II $\tau_{xy})_{y=0}\neq 0$ (3)

Where $P_U(x)$ represents the distribution of load intensity applied on the top surface of the upper layer. Equations (3) are to be addressed later.

Considering the aforementioned boundary conditions, integral transforms (**APPENDIX (A)**) for stress and displacement components included in solutions to elastic problems are as seen in Equations (4).

$C_j[v)_{x=L}]=C_j[v)_{x=0}]=A_j$, $C_m[u)_{y=h}]=B_m$, $C_m[u)_{y=0}]=B_m'$, $S_m[\sigma_y)_{y=h}]=D_m$, $S_m[\sigma_y)_{y=0}]=D_m'$ (4)

Where A_j, B_m, B_m', D_m, and D_m' represent the unknown boundary quantities, with $j,m=1,2,3\cdots$. Then, general equations for stress and displacement components that include these unknown boundary quantities turns out to be:

$$u=-\frac{1}{2h}\sum_j \sin Jy\Big[\Big\{F^{(0)}(Jx)-G^{(0)}(Jx)\Big\}-\nu\Big\{F^{(2)}(Jx)-G^{(2)}(Jx)\Big\}\Big]A_j-\frac{1}{2L}\sum_m \cos Mx\Big[\Big\{2\alpha^Q(My)-(1+\nu)\beta^P(My)\Big\}B_m-\Big\{2\alpha^Q(My)-(1+\nu)\alpha^P(My)\Big\}B_m'+\frac{(1+\nu)^2}{EM}\Big\{\beta^P(My)D_m-\alpha^P(My)D_m'\Big\}\Big] \quad (5)$$

$$v=\frac{1}{2h}\sum_j \sin Jy\Big[2\Big\{\alpha^Q(Jx)-\beta^Q(Jx)\Big\}-(1+\nu)\Big\{\alpha^P(Jx)-\beta^P(Jx)\Big\}\Big]A_j-\frac{1}{2L}\sum_m \sin Mx\Big[\Big\{G^{(0)}(My)-\nu G^{(2)}(My)\Big\}B_m-\Big\{F^{(0)}(My)-\nu F^{(2)}(My)\Big\}B_m'-\frac{1+\nu}{EM}\Big\{2G^{(0)}(My)+(1-\nu)G^{(2)}(My)\Big\}D_m+\frac{1+\nu}{EM}\Big\{2F^{(0)}(My)+(1-\nu)F^{(2)}(My)\Big\}D_m'\Big]+v_0 \quad (6)$$

$$\sigma_x=\frac{E}{2h}\sum_j J\cdot\sin Jy\Big\{\beta^P(Jx)-\alpha^P(Jx)\Big\}A_j+\frac{1}{2L}\sum_m \sin Mx\Big[EM\Big\{2\beta^Q(My)-\beta^P(My)\Big\}B_m-EM\Big\{2\alpha^Q(My)-\alpha^P(My)\Big\}B_m'+\Big\{(1+\nu)\beta^P(My)-2\nu\beta^Q(My)\Big\}D_m-\Big\{(1+\nu)\alpha^P(My)-2\nu\alpha^Q(My)\Big\}D_m'\Big] \quad (7)$$

$$\sigma_y=\frac{E}{2h}\sum_j J\cdot\sin Jy\Big[-\Big\{\beta^P(Jx)-\alpha^P(Jx)\Big\}+2\Big\{\beta^Q(Jx)-\alpha^Q(Jx)\Big\}A_j\Big]+\frac{1}{2L}\sum_m \sin Mx\Big[EM\Big\{\beta^P(My)B_m-\alpha^P(My)B_m'\Big\}-\Big\{(1+\nu)\beta^P(My)+2\beta^Q(My)\Big\}D_m-\Big\{(1+\nu)\alpha^P(My)+2\alpha^Q(My)\Big\}D_m'\Big] \quad (8)$$

$$\tau_{xy}=-\frac{E}{2h}\sum_j J\cdot\cos Jy\Big[\Big\{F^{(2)}(Jx)-G^{(2)}(Jx)\Big\}A_j+\frac{1}{2L}\sum_m \cos Mx\Big[EM\Big\{G^{(2)}(My)B_m-F^{(2)}(My)B_m'\Big\}+\Big\{G^{(0)}(My)-\nu G^{(2)}(My)\Big\}D_m-\Big\{F^{(0)}(My)-\nu F^{(2)}(My)\Big\}D_m'\Big] \quad (9)$$

In the above equations, α^P, α^Q, β^P, β^Q, $F^{(0)}$, $F^{(2)}$, $G^{(0)}$, and $G^{(2)}$ are the sum of infinite series of the Fourier transforms, as shown in **APPENDIX (B)**. J is equal to $j\pi/L$, M is equal to $m\pi/L$, and v_0 is obtained from $v)_{x=L_1,y=0}$.

(2) Determination of Unknown Quantities of Boundary

The five unknown quantities of boundary are identified by solving five simultaneous equations: the second equation in Equations (1), 2 equations in Equations (2), and 1 equation in Equations (3), plus the conditional equation (the differential

equation of the beam theory), assuming that displacement on the interface between the upper and the lower layers are continuous.

As mentioned above, there are two cases for Equations (3): CASE I , where friction was not caused on the interface, and CASE II , where friction occurs on the interface. For CASE I , Equation (9) should substitute for the left term of the first equation in Equations (3). The differential equation of the beam theory in this case is as follows.

$$E_s I_s \frac{d^4 v)_{y=0}}{dx^4} = \sigma_y)_{y=0} - P_L(x) \tag{10}$$

Note that $P_L(x)$ in the equation is the load distribution intensity on the bottom surface of the lower layer, while I_s represents the moment of inertia on the section of the beam constituting the lower layer, which is equal to $h_s^3/12$.

CASE II is further divided into two sub-cases: CASE II-1, where the upper and the lower layers are completely bonded to each other, and CASE II -2, where some friction is caused between them. In CASE II-1, the equilibrium of shearing force T and axial force N on the interface is:

$$dT + N = 0 \tag{11}$$

and dT and N are represented by

$$dT = \tau_{xy}) \cdot dx$$
$$N = E_s h_s \frac{du)_{y=0}}{dx} \tag{12}$$

Hence the second equation in Equations (3) results in:

$$\tau_{xy})_{y=0} = -E_s h_s \frac{d^2 u)_{y=0}}{dx^2}$$
$$= \frac{2}{L} E_s h_s \sum_m \cos Mx \cdot M^2 \cdot B_m' \tag{13}$$

In CASE II-2, when the shearing force on the bottom surface of the upper layer is assumed to be proportionate to the difference between displacement in x direction of the upper and that of the lower layers that are observed on the interface, the relationship between them is indicated by the following equation.

$$\tau_{xy})_{y=0} = k\{u)_{y=0} - u_0\} \tag{14}$$

Where k, called the "spring constant" in this paper, is a constant with load intensity dimension for a unit length. Therefore, no friction occurs on the interface when k=0, whereas the upper and the lower layers are completely bonded when k=∞, as derived from Equation (14). The difference in the k value represents the difference in the magnitude of friction on the interface. For u_0, which is displacement in x direction on the top surface of the lower layer, the following relationship is formed as the shearing force on the bottom surface of the upper layer is equal to that on the top surface of the lower layer.

$$E_s h_s \frac{d^2 u_0}{dx^2} = -\tau_{xy})_{y=0} \tag{15}$$

When Equation (14) is differentiated twice to be followed by the substitution with Equation (15), the result is:

$$\frac{d^2 \tau_{xy})_{y=0}}{dx^2} - \frac{k}{E_s h_s} \tau_{xy})_{y=0} = k \frac{d^2 u)_{y=0}}{dx^2} \tag{16}$$

Thus the following equation is obtained for CASE II-1:

$$\tau_{xy})_{y=0} = \sum_m \cos Mx \cdot C_m$$

When this is substituted in Equation (16) to determine unknown number C_m, the second equation in Equations (3) becomes:

$$\tau_{xy})_{y=0} = \frac{2}{L} \sum_m \cos Mx \frac{kM^2}{M^2 + k/(E_S h_S)} B_m' \tag{17}$$

For both CASE II-1 and CASE II-2, the differential equation for the beam theory turns out to be:

$$E_s I_s \frac{d^4 v)_{y=0}}{dx^4} = \sigma_y)_{y=0} - P_L(x) - \frac{h_s}{2} \frac{d\tau_{xy})_{y=0}}{dx} \tag{18}$$

When it is assumed that steel rods are used for the loading point and the support in **Fig. 1** and that they constitute parabolic loads with load distribution width $2L'$, the equations indicated below are formed for $P_U(x)$ and $P_L(x)$, which are the load intensity distribution of the top and the bottom surfaces respectively.

$$P_U(x) = \frac{2}{L} \sum_m \frac{3P(1 - (-1)^m)}{(ML')^2} \left\{ \frac{\sin ML'}{ML'} \right.$$

Table 1 Dimensions of analyzed model for numerical computation. (b=1cm)

Dimensions	L/b	4
	L_U	0.375L
	L_L	0.125L
	L'	0.005L
	h_0	0.0025～0.01L
	h	0.1～0.25L
Mechanical properties	E_S/E	1～1000
	ν	0.3
	k	0～∞

Table 2 Precision of computed shearing stress on boundary faces.

x／L		0.0	0.25	0.5	0.75	1.0
$\tau_{xy})_{y=h}/q$	CASE I	−0.00001	0.00000	0.00000	0.00000	0.00001
	CASE II-2 (k=0)	−0.00001	0.00000	0.00000	0.00000	0.00001
	CASE II-1	−0.00009	0.00000	0.00000	0.00000	0.00009
	CASE II-2 (k=∞)	−0.00009	0.00000	0.00000	0.00000	0.00009
$\tau_{xy})_{y=0}/q$	CASE I	−0.00000	0.00000	0.00000	0.00000	0.00000
	CASE II-2 (k=0)	−0.00000	0.00000	0.00000	0.00000	0.00000
	CASE II-1	−0.00011	0.03041	0.00000	−0.03041	−0.00011
	CASE II-2 (k=∞)	−0.00011	0.03058	0.00000	−0.03058	−0.00011
y／h		0.0	0.25	0.5	0.75	1.0
$\tau_{xy})_{x=0}/q$	CASE I	−0.00000	−0.00001	−0.00001	−0.00001	−0.00001
	CASE II-2 (k=0)	−0.00000	−0.00001	−0.00001	−0.00001	−0.00001
	CASE II-1	−0.00011	−0.00011	−0.00011	−0.00011	−0.00009
	CASE II-2 (k=∞)	−0.00011	−0.00011	−0.00011	−0.00011	−0.00009

$$- \cos ML' \Big\} \sin ML_U \sin Mx \qquad (19)$$

$$P_L(x) = \frac{2}{L} \sum_m \frac{3P(1-(-1)^m)}{(ML')^2} \left\{ \frac{\sin ML'}{ML'} - \cos ML' \right\} \sin ML_L \sin Mx \qquad (20)$$

3. VALUE CALCULATIONS

(1) Accuracy and Applicability of Calculations

Table 1 shows conditions for calculations made by a personal computer (CPU: Pentium processor 166 MHz, program language: C++). In matrices for calculations through the simultaneous equations, m and n are set to be 300 terms for each. Calculation accuracy is determined depending on whether or not the boundary conditions in Equations (1) through (3) can be satisfied. Of these, the first and the second equations in Equations (1) are basically satisfied through Equations (6) and (7) and **APPENDIX (B)**, but it is difficult to satisfy other conditional equations due to limitations in computations for the series. With h, h_s, and E_s/E set $0.25L$, $0.005L$, and 100 respectively, the shearing stress of the boundary surface is divided by load frequency q in order to see whether or not the conditions are satisfied. The **Table 2** shows that variation of τ_{xy}/q with x/L and in the periphery τ_{xy} nearly vanishes. It can be said the boundary conditions are well satisfied in these two cases, CASE I and CASE II-2 (k=0) where no friction is on the interface.

In CASE II-1 and CASE II-2 (k=∞), where the upper and the lower layers are completely bonded to each other, the boundary conditions are almost satisfied with regard to the top and the side

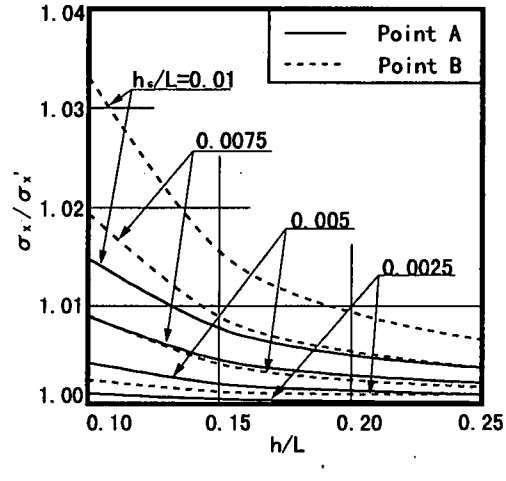

Fig.2 Effect of h_s/L on σ_x in central section.

surfaces, while symmetrical shearing stress occurred on the cross section at the center of the span of the interface.

As indicated in (2) in Chapter 2, the beam theory was applied to the conditional equation representing the continuous displacement of the upper and the lower layers at their interface, as well as to the conditional equation concerning shearing strength. In other words, the lower layer takes the form of a beam to which the beam theory is applicable. When an elastic analysis is conducted for the two layers, the results of such analysis may not necessarily coincide with the results obtained from the present analysis because of the thickness of the lower layer. Therefore, in an attempt to evaluate the stress and displacement in CASE II-1, a comparison was made between the results of two cases with different calculations: one in which the elastic coefficient of the upper

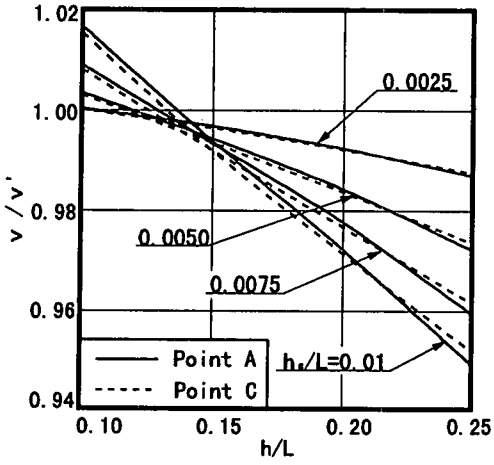

Fig.3 Effect of h_s/L on vertical displacement on top face.

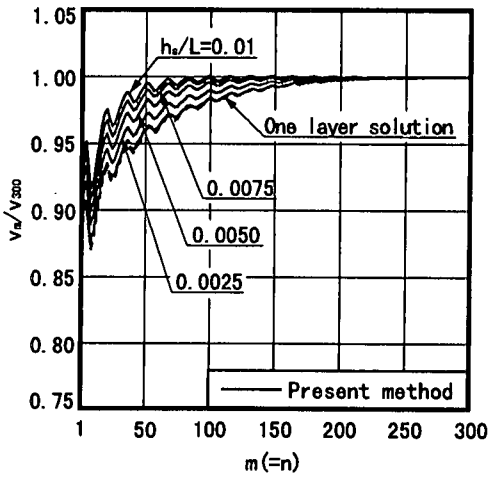

Fig.4 Convergent conditions on vertical displacement.

and the lower layers is assumed to be E_s/E=1 according to the results of the present analysis, and the other in which h_s+h was used as the thickness of the beam according to the analysis result of Reference 5), while employing values identical with the present calculation for the length and for the mechanical properties associated with elasticity of the specimen (hereunder called the "one-layer analysis).

Fig. 2 presents the results of σ_x/σ_x', a ratio between σ_x, stress in CASE Ⅱ-1, and σ_x', stress from one-layer analysis [5]. Horizontal stress in points A and B are examined by changing h/L, the thickness of the upper layer. The difference between σ_x/σ_x' and 1 indicates an analytical error between the result of this analysis and strict solution. When the thickness of the lower layer remains constant, σ_x/σ_x' decreases as the upper layer becomes thicker. In other words, analytical errors increase as the upper layer becomes thinner. The fact that the analytical error is larger at the bottom surface is believed to reflect the influence upon the assumption of the straight beam for the lower layer, because the percentage of the lower layer in the total thickness increases as the thickness of the upper layer is reduced, provided that h_s/L is small.

Fig. 3, on the other hand, shows the results of similar investigations into analytical errors that were obtained in the form of v/v', where v is vertical displacement at point A and point C in **Fig. 1**, while v' represents vertical displacement derived from one-layer analysis. When h_s/L is within a range from 0.025 to 0.01, the figure indicates that the largest analytical error is close to 5%, much more significant than errors for stress. Note that the error also increases in proportion to

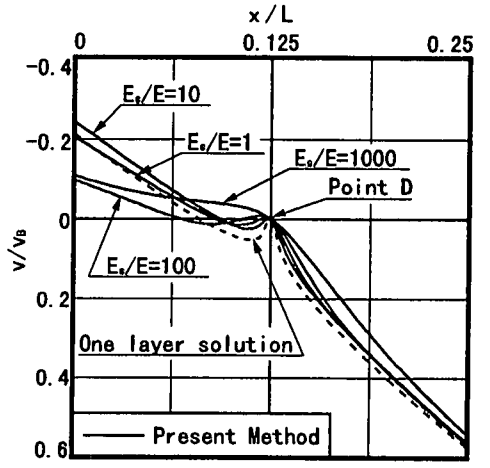

Fig.5 The local deformation on bottom face. (h_s/L=0.005, h/L=0.25)

h/L. This presents a contrast to the tendency observed with respect to stress components. When h_s/L=0.005, for example, the analytical error of stress components is relatively small, but the error of displacement components is nearby 3%. In relation to this fact, **Fig.4** illustrates the convergence condition concerning the vertical displacement of the upper central part. For both m and n, results are represented as the ratio of v_{300} (displacement with respect to 300 terms) to v_m (calculation results for respective terms). In both the results of the present analysis and the results of one-layer analysis, computations for the series are converged almost completely in less than 300 terms. The errors therefore are not attributed to calculation but are probably due to the application

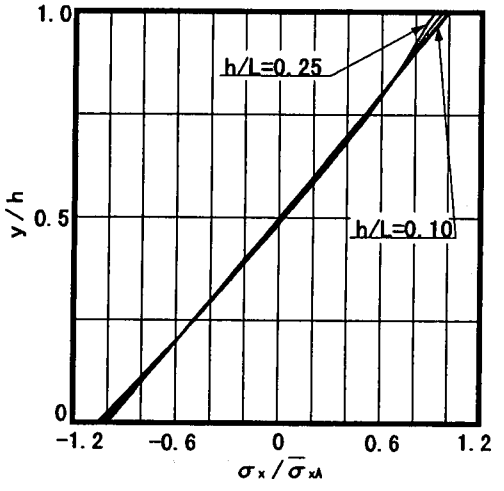

Fig.6 Distribution of σ_x along central section. (CASE I)

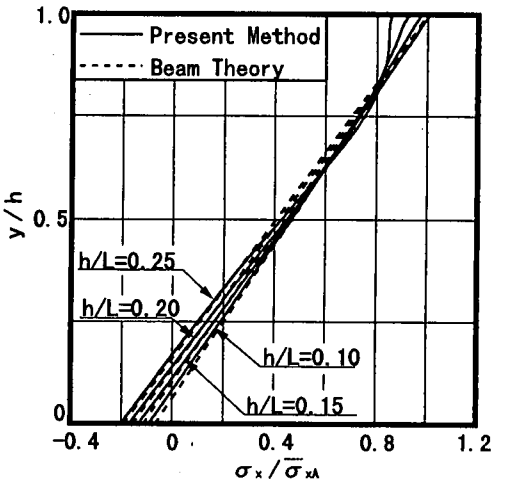

Fig.7 Distribution of σ_x along central section. (CASE II-1)

of Equation (10) and Equation (18) for the continuity between the upper and the lower layers, although the cause of the errors cannot be clearly identified.

On a two-dimensional plane in rectangular coordinates, the influence of shearing force on deflection takes the form of local deformation [10] of the loading point and the support [5]. As **Fig. 5** shows, studies were conducted on deflections due to local deflection of support, by dividing v (displacement of the bottom of the lower layer) by v_B (deflection on point B in **Fig. 1**). When a comparison is made between the results of the present analysis and the results of one-layer analysis under the condition that the upper layer and the lower layer have the same elastic coefficient, the difference of deflections becomes obvious near the support. According to **Fig. 5**, however, the deflection caused by local deformation is gradually reduced as E_S/E increases in accordance with the rigidity of the lower layer. Consequently, the effect of shearing force is expected to diminish as the rigidity of the lower layer becomes higher. Since the results of the present analysis are deemed applicable when the rigidity of the lower layer is higher than the rigidity of the upper layer, the analytical error of about 3% in **Fig. 5** is not so serious as to prevent us from applying the analysis results of displacement components to the evaluation of elasticity of pavement mixture.

Based on the above, it is considered that the results of the present analysis are applicable when the thickness of the lower layer is not more than 0.5% of the total length of the beam, provided that h/L is between 0.1 to 0.25. The sizes of the test specimens and the steel plate that were used in the experiments by Himeno et al. were 0.13 in h/L and 0.005 in h_s/L with the beam length of 30 cm [3].

(2) Calculation Results

a) Horizontal Stress

Discrepancy is observed between the results from the beam theory and those from elastic analysis, with regard to stress in x direction that is derived from one-layer analysis [5),11)]. According to increases in h/L, the discrepancies between them become clearer on the top and the bottom surfaces. It is now known that the disparity is not due to a difference in elastic modulus E or Poisson's ratio [5),11)]. On the other hand, Equation (21) [8)] is formed for $\bar{\sigma}_x$, stress in x direction at the central cross-section being derived from the beam theory for a two-layered structure. It is readily anticipated that the results calculated through this equation will be different from those obtained from the present analysis in Chapter 2.

$$\bar{\sigma}_x = \frac{P(L-L_U-L_L)}{IE+I_SE_S}y' \tag{21}$$

Where, for CASE I,

$$y' = h/2 - y \qquad I = h^3/12 \qquad I_s = h_s^3/12 \tag{22}$$

and for CASE II,

$$y' = y_N - h_s - y \qquad y_N = \frac{Eh^2+E_Sh_S^2+2Ehh_S}{2(Eh+E_Sh_S)}$$

$$I = \frac{h^3}{12} + h\left(y_N - \frac{2h+h_s}{2}\right)^2 \qquad I_s = \frac{h_s^3}{12} + h_s\left(y_N - \frac{h_s}{2}\right)^2 \tag{23}$$

Both **Fig. 6** and **Fig. 7** illustrate a manner in

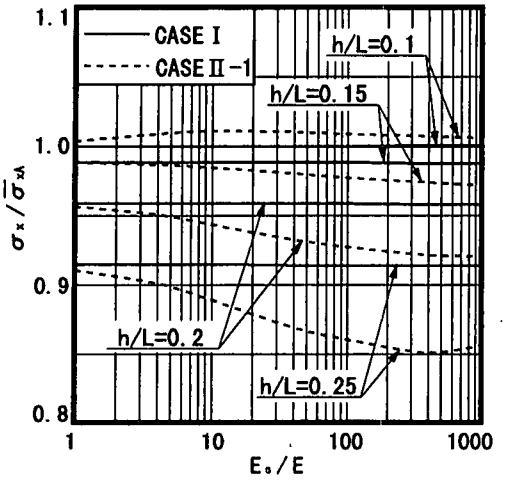

Fig.8 Effect of E_s/E on σ_x in central section.

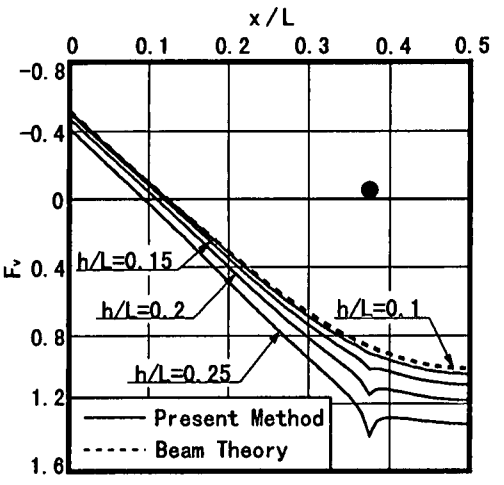

Fig.9 Deflection on top face. (CASE I)

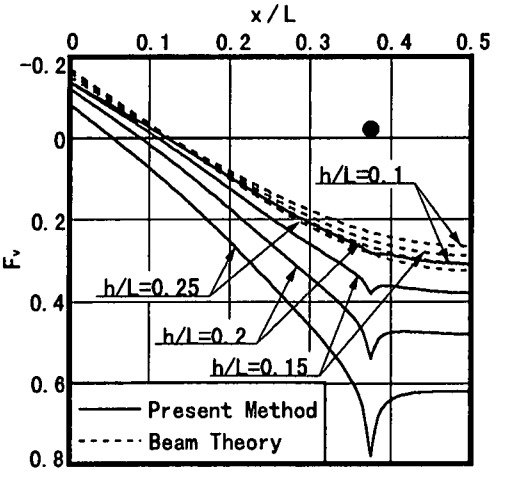

Fig.10 Deflection on top face. (CASE II-1)

which σ_x, stress in x direction, is distributed over the central cross-section of the upper layer when E_s/E is equal to 100. **Fig. 6** presents solutions for CASE I, and **Fig. 7** concerns the calculation results for CASE II. These figures also indicate the ratio of σ_x to $\overline{\sigma}_{xA}$, which was determined by dividing σ_x, stress in x direction that was obtained from the present analysis, by $\overline{\sigma}_{xA}$, stress on point A in **Fig. 1** as derived from the beam theory in Equation (21). Therefore, the results of calculation based on the beam theory are also seen in the two figures.

As **Fig. 6** demonstrates, when layer thickness accounts for 10% of beam length, the stress distribution resulting from the calculation for CASE I is almost identical with the distribution derived from the beam theory, and no difference can be seen in the figure. Stress determined through the beam theory is scarcely affected by difference in thickness, but stress determined by elastic analyses of the top and bottom surfaces varies by several percent, according to the layer thickness. This coincides with the tendency of stress distribution that was identified assuming the single layer [5),11)].

In contrast, **Fig. 7** for CASE II shows a notable difference between the results from the present analysis and the results from the beam theory. On the top surface, in particular, deviation from the stress calculated through the beam theory becomes more pronounced as the layer thickness increases, while variation in the thickness does not significantly affect the degrees of difference between the two approaches.

The ratio of σ_x to $\overline{\sigma}_{xA}$ is further examined by changing E_s/E, as illustrated in **Fig. 8**. In CASE I, the difference in the ratio $\sigma_x/\overline{\sigma}_{xA}$ remained almost unchanged regardless of the rigidity ratio of the upper and the lower layers, while the difference in $\sigma_x/\overline{\sigma}_{xA}$ is inconsistent as the rigidity of the lower layer rose in CASE II-1.

The above-mentioned investigations have made it clear that stress in x direction in the upper layer is affected by the size of the specimen, the bonding condition of the two layers along the interface, and the elastic coefficients of the upper and the lower layers.

b) Surface Deflection

Fig. 9 and **Fig. 10** indicate deflection distribution over the top surface of the upper layer under the condition of E_s/E=100. Calculation results in **Fig. 9** are concerned with CASE I, whereas **Fig. 10**

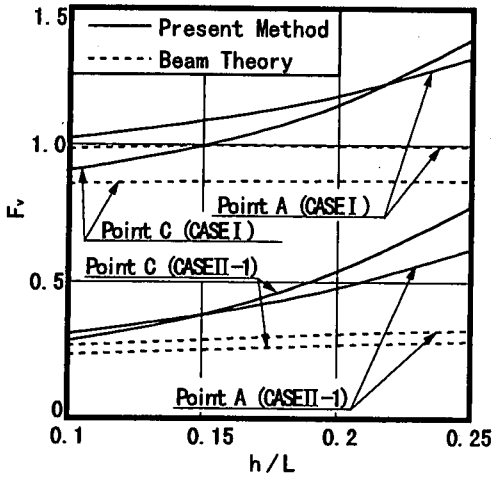

Fig.11 Relationship between the deflection on top face and h/L. (E_S/E=100)

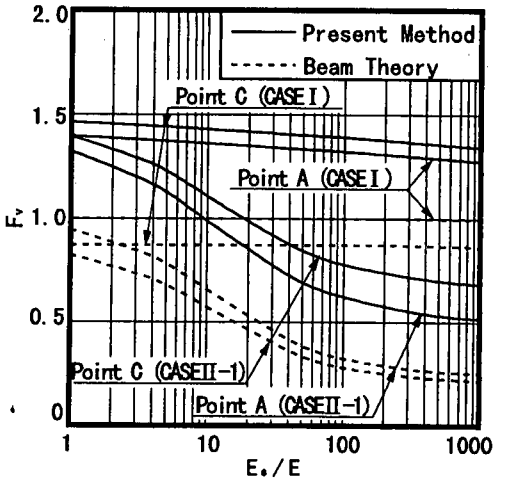

Fig.12 Relationship between the deflection on top face and E_S/E. (h/L=0.25)

presents deflection distribution in CASE II-1. These results for the two cases are presented in the form of F_v, i.e., the ratio of analysis displacement v in Equation (24) below to the center displacement in a single layer, which is based on the beam theory.

$$F_v=\frac{2Eh^3}{P(L_U-L_L)\{3(L-2L_L)^2-4(L_U-L_L)^2\}}\cdot v \qquad (24)$$

The figures also include calculation results through the beam theory. These deflections are represented by the following equation.

$$v=\frac{P(L_U-L_L)}{12(EI+E_SI_S)}\left\{8(L_U-L_L)^2+3(L-2L_U)(L+2L_U-4L_L)\right\} \qquad (25)$$

In the equation above, I and I_S correspond to Equation (22) in CASE I and Equation (23) in CASE II-1, respectively.

As is clear from the above, when the thickness of the upper layer was small, there was little difference in deflection between the present analysis and the beam theory, while the difference became greater as the thickness increased. This was always the case irrespective of the difference in boundary conditions of the interface. Moreover, an increase in the thickness of the upper layer caused local deformation to appear directly below the loading point. This tendency was also observed in the results of calculation based on the assumption for a single layer [5].

For points A and C in **Fig. 1**, investigations were made on changes in F_v that occur with variations in the thickness of the upper layer. **Fig. 11** shows the results of these investigations, as well as the results of calculation relying on the beam theory. Regardless of the boundary conditions, deflection becomes larger as the thickness of the upper layer increases, widening a gap between the present analysis and the beam theory. Note that the rate at which deflection increases is not much affected by difference in boundary conditions, although the rate of increase in deflection varies from the center to the loading point when the boundary conditions are the same. When the thickness of the upper layer exceeds a certain level, deflection due to the local deformation at the loading point becomes markedly larger, exceeding deflection at the center. Particularly, when the two layers are completely bonded to each other across the interface, the deflection attributed to local deformation at the center increases while the upper layer is still thinner than in the case where friction is not observed.

Fig. 12 illustrates changes in F_v at points A and C in **Fig. 1** that are caused by variation in E_S/E, when h/L=0.25. The figure also shows the results of a calculation based on the beam theory. When the rigidity of the lower layer becomes higher than that of the upper layer, deflection is reduced. The rate at which deflection decreases varies depending on boundary conditions and positions, i.e., the loading point vs. the center. In CASE I, the difference in F_v between the two positions in particular has been found to be hardly affected by variations in E_S/E. This is also the case with the results of calculations relying on the beam theory. In CASE II, on the other hand, the difference in F_v between the center and the loading point

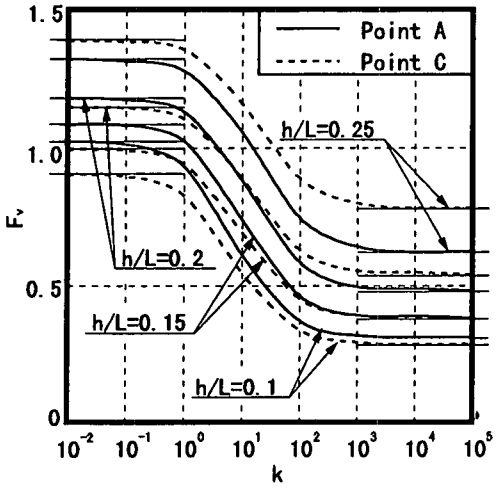

Fig.13 Relationship between the deflection on top face and spring constant k for various h/L-values. (E_s/E=100)

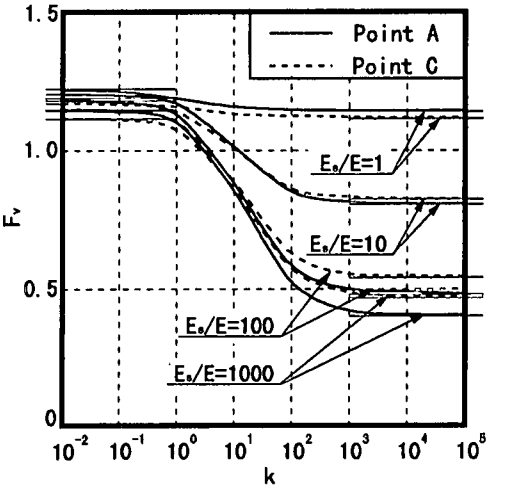

Fig.14 Relationship between the deflection on top face and spring constant k for various E_s/E-values. (h/L=0.2)

depends to a significant degree on variations in E_s/E. Furthermore, according to elastic analysis, the difference in F_v between the two points becomes larger as E_s/E increases, while it diminishes with an increase in E_s/E when the beam theory is adopted. The results of the present analysis demonstrate that in the case where the upper and the lower layers are completely bonded to each other across the interface, local deformation of the loading point becomes larger as the difference in deflection between point A and point C augments against the increases of E_s/E .

The above-mentioned results reveal that the scale of deflection is affected by the thickness of the upper layer, the rigidity ratio, and the conditions of the boundary surface. However, the calculations involving the status of the boundary were carried out based on the assumption of two extremes: boundary where no friction is found, and a boundary along which the layers are completely bonded to each other. Neither of them was considered a actual condition under which a loading test was conducted. In view of this unlikelihood, the effects of varying friction on deflection were examined through the calculation CASE Ⅱ-2.

Fig. 13 shows changes in F_v at points A and C in **Fig. 1** as they occur for different levels of h/L when spring constant k varies. The F_v values corresponding to k=0 and k=∞ are indicated by extended horizontal lines. As the figure demonstrates, deflection is reduced as spring coefficient k increases, but the rate of reduction is not much affected by variations in layer thickness, as long as positions for calculation remain within the same coordinates. Spring constants for F_v values similar to those corresponding to k=0 and k=∞ are $10^{-2} \leqq k$ and $10^3 \geqq k$, respectively, and changes in F_v are most pronounced when k is within a range from 10^0 and 10^3. On the other hand, a difference is observed between the center and the loading point as to the rate at which deflection decreases according to increases in spring coefficients. When h/L=0.2, for example, deflection at the loading point is larger than deflection at the center, due to the effect of local deformation. Such differences in the scale of deflection are more notable when h/L is larger.

Fig. 14 shows changes in F_v at points A and C in **Fig. 1** as they occur for different levels of E_s/E when spring coefficient k varies. The F_v values corresponding to k=0 and k=∞ are indicated by the extended lines of the horizontal axis. As the figure demonstrates, deflection is reduced as spring coefficient k increases, and the rate of reduction is significantly affected by variations in E_s/E. Spring coefficients for F_v values similar to those corresponding to k=0 and k=∞ are $10^{-2} \leqq k$ and $10^3 \geqq k$, respectively, and changes in F_v are most striking when k is within a range from 10^0 and 10^3. On the other hand, a difference is observed between the center and the loading point as to the rate at which deflection decreases according to increases in spring coefficients. When E_s/E is 10 or more, for example, deflection at the loading point is larger than deflection at the center, due to the effect of local deformation. Such differences in the scale of deflection are more pronounced when E_s/E is larger. According to the results from **Fig. 13** and **Fig.14**, the spring coefficient of k should

be established before determining the mechanical property of asphalt mixture. Although it is difficult to obtain k through experiments, parameters E and k that need to be determined can be simultaneously defined by conducting two loading tests in which the sizes of specimens and the thickness and properties of steel plates differ from each other, as Reference 6) indicates. Consequently, the results from the two figures will serve as basic materials to help identify the degree of friction based on the k value.

4. CONCLUSION

As reported in this paper, models were constructed for bending tests by using the specimens of pavement mixture on a thin steel plate, with a view to carrying out two-dimensional elastic analysis for such a two-layer plate and beam structure. However, this approach called for inquiries into the applicability of the results of such analysis, due to the fact that a differential equation of the beam theory was applied for the continuity condition of the load and displacement of the lower layer. Investigations have made it clear that the results of the present analysis is sufficiently accurate when the thickness of the upper layer is between 0.1 and 0.25L and when the thickness of the lower layer does not exceed 0.05L. Then, a series of calculations was made to identify factors in the analysis that might affect differences in deflection when the analysis results described in this paper are employed for evaluating the elasticity of the asphalt mixture, resulting in the following findings.

(1) When the length of a beam was the same, deflection was considerably affected by the thickness of the upper layer, the bonding conditions of the upper and the lower layers, and differences in rigidity between the two layers.

(2) According to the results of the analysis in which spring constant was employed, the difference in friction between the upper and the lower layers had no small effect on deflection. The range of spring constant affecting deflection the most was found to be from 10^0 to 10^3.

(3) When the beam length was the same, deformation on the loading point increased according to increases in friction over the interface and/or rigidity ratio between the upper and the lower layer.

Comparisons between the numerical computation of stress in x direction and the values based on the beam theory demonstrated that the extent to which the two types of analysis differ from each other depends on variations in the bonding conditions of the layers and the rigidity. As a consequence, close attention should be paid to strain measurement when the results of such measurement are to be used together with the outcome of stress analysis in order to determine the constant of the material. It is also necessary to be able to identify the bonding status of the interface. Since the time required for the computation of one condition is only about 5 minutes, this analysis program may well be practically applied. Nonetheless, in the tests for determining mechanical property, where the same sized specimens were used, the application of the results of the present analysis gave rise to the problem of enlarged local deformation, because the stiffness ratio between the upper and the lower layers in case of the test piece of higher temperature. This is likely to be accompanied by an increase in $2L'$, the load distribution width on the loading point. Methods for applying the results of the present analysis and actual examples of the application have yet to be discussed in a separate paper. In pursuing this subject, in-depth analyses and experiments should be conducted on the aforementioned issues and on the effects of friction over the layer boundary surface.

APPENDIX [12]

(A) Integral Conversion

When $f(x)$ is a continuum between 0 and L, the finite Fourier transforms of $f(x)$ is expressed by the following equation.

$$S_m[f(x)] = \int_0^L f(x)\sin Mx\,dx$$

$$C_m[f(x)] = \int_0^L f(x)\cos Mx\,dx$$

(B) Sum of Infinite Fourier Series

$$\alpha^P = P^{(1)} + P^{(2)} \qquad \alpha^Q = Q^{(1)} + Q^{(2)}$$

$$\beta^P = -P^{(1)} + P^{(2)} \qquad \beta^Q = -Q^{(1)} + Q^{(2)}$$

$$\left.\begin{matrix} F^{(0)} \\ G^{(0)} \end{matrix}\right\} = \pm\left\{(\phi^{(1)}+\psi^{(1)}) \pm(\phi^{(2)}+\psi^{(2)})\right\}$$

$$\left.\begin{matrix} F^{(2)} \\ G^{(2)} \end{matrix}\right\} = \pm\left\{(\phi^{(1)}-\psi^{(1)}) \pm(\phi^{(2)}-\psi^{(2)})\right\}$$

$$\left.\begin{matrix} P^{(1)}(\xi r) \\ P^{(2)}(\xi r) \end{matrix}\right\} = \frac{\xi\{r\,\mathrm{sh}\xi(l-r) \pm (l-r)\,\mathrm{sh}\xi r\}}{\mathrm{ch}\xi l \pm 1}$$

$$\left.\begin{matrix} Q^{(1)}(\xi r) \\ Q^{(1)}(\xi r) \end{matrix}\right\} = \frac{\mathrm{ch}\xi(l-r) \pm \mathrm{ch}\xi r}{\mathrm{ch}\xi l \pm 1}$$

$$\left.\begin{matrix}\phi^{(1)}(\xi r)\\ \phi^{(2)}(\xi r)\end{matrix}\right\}= \frac{\mathrm{sh}\xi(l- r)\mp\mathrm{sh}\xi r}{\mathrm{ch}\xi l\pm 1}$$

$$\left.\begin{matrix}\psi^{(1)}(\xi r)\\ \psi^{(2)}(\xi r)\end{matrix}\right\}= \frac{\xi\{r\mathrm{ch}\xi(l- r)\mp(l- r)\mathrm{ch}\xi r\}}{\mathrm{ch}\xi l\pm 1}$$

In the above equations, sh x and ch x represent hyperbolic functions sinh x and cosh x, respectively. If ξ is M, r is replaced by y and l by h; if ξ is J, r and l are replaced by x and L, respectively.

REFERENCES

1) Research Group of Asphalt Pavement Technology : Canges of Asphalt Pavement Technology, *ASPHALT*, No.155/Vol-30, pp.5-21, 1988.

2) Hass, R. and Hudson, W. R. : Pavement Management Systems , *McGRAW-HILL*, 1978.

3) Himeno, K., Watanabe, T. and Maruyama, T. : Fatigue Failure Characteristics of Asphalt Mixes at Low Stiffness Modulus, *Journal of Materials, Concrete Structures and Pavements, JSCE*, Vol.4, No.235, pp.143-151, 1986.

4) For example,
Kasahara, A. and Sugawara, T. : Canges of Dynamic Properties of Bituminous Mixtures under Repeated Loading, *Proceedings of The JSCE*, No.235, pp.87-98, 1975.

5) Kuriyagawa, Y., Akiba, S., Kida, T. and Nomachi, S. G. : Elastic Analysis of Pavement Materials with the Bending Test by Two Points Loading, *Journal of Materials, Concrete Structures and Pavements, JSCE*, Vol.33, No.550, pp.211-220, 1996.

6) Kuriyagawa, Y., Akiba, S., Kida, T. and Nomachi, S. G. : A study on Estimation of the Mechanical Properties of Pavement Materials by the Repeated Bending Test, *Journal of Materials, Concrete Structures and Pavements, JSCE*, Vol.35, No.564, pp.211-220, 1997.

7) Kuriyagawa, Y., Akiba, S., Kida, T. and Nomachi, S. G. : Development and Application of a Determining Method of Complex Modulus for Fatigue of Pavement Mixture, *Journal of Structural Engineering, JSCE*, Vol.43A, pp.21-30,1997.

8) Mogami, T. : Applied Mechanics (Fourth Edition), *Kinbar-Shuppan*, Tokyo, Japan, 1971.

9) Nomachi, S. G. : On Applications of Finite Fourier Transformation to Problems in Thin Plate and plane Elasticity, *Journal of Muroran Institute of Technology*, Vol.2, No.2, pp123-141, 1956.

10) Timoshenko, S. P. and Goodier, J. N. : Theory of Elasticity (Third Edition), *McGRAW-Hill*, pp.46-50, pp.113-122,1970.

11) Watanabe, S. and Kishi, T. : Considerations by Elastic Analysis on the Cracking Position of Brittle Beam Induced by Third-Point Loading Test, *Transactions of the JSIDRE*, No.163, pp.19-27, 1993.

12) Nomachi, S.G.: One Method of Solving Stress Problem in Cylindrical Co-ordinates by Means of Finite Fourier Hankel Transforms (Part I), *Memories of Muroran Institute of Tech.* Vol.3, No.3, pp.91-115, 1960.

(Received April 15, 1998)

はり上にあるアスファルト混合物の２次元弾性解析

秋葉正一・栗谷川裕造・能町純雄・秋山成興

本論文は，低スティフネス状態における初等曲げ理論の適用不可能な形状を有するアスファルト混合物供試体が，薄いスチール板上にある場合の曲げ試験を想定し，このような2層構造における供試体の2次元弾性解析を実施した結果を述べたものである．本解析では層境界面における摩擦の影響を考慮した境界条件を設定し，解析手法の妥当性および解析結果の適用範囲を数値計算により検討した結果，本解析結果の有用性が確認できた．また，数値計算結果では，混合物の弾性的評価を行うために必要不可欠な材料定数の推定を変位の測定結果と変位成分の解析結果を用いて実施する上で，解析変位に影響を与える供試体形状，上下境界面の摩擦および上下層の弾性係数比などの基礎情報を得た．